Journal of Physics: Conference Series **525** (2014) 012016 doi:10.1088/1742-6596/525/1/012016

In Situ Testing of Metal Micro-Textured Thermal Interface Materials in Telecommunications Applications

R Kempers[1,3] and S Kerslake[2]

[1]Alcatel-Lucent Ireland, Wireless Advanced Technologies, Blanchardstown Business & Technology Park, Dublin 15, Ireland
[2]Alcatel-Lucent Telecom, Swindon, United Kingdom
[3]Department of Mechanical and Manufacturing Engineering, Parsons Building, Trinity College Dublin

Email: kempersr@tcd.ie

Abstract. A metal micro-textured thermal interface material (MMT-TIM) has been developed to address the shortcomings of conventional TIMs for Remote Radio Heat (RRH) applications. The performance of the MMT-TIM was characterized in-situ by monitoring the temperatures of the dominant heat generating devices in an RRH Power Amplifier for a fixed input power. Measurements show that the use of the MMT-TIM results in significantly lower devices temperatures than achieved with the conventionally used graphite pads with a maximum temperature drop of 14.9 °C observed. The effect of power cycling on the long term performance trends is also examined.

1. Introduction

The mitigation of thermal contact resistance is essential to the performance of conduction-based electronic thermal management solutions which are employed in numerous ICT applications. Typically the most feasible strategy to reduce thermal contact resistance is to insert a thermal interface material (TIM) of higher thermal conductivity between the mating surfaces to conform to the contacting surface asperities and displace any micro and macroscopic air voids, thereby providing an improved path for heat transfer between the two components.

To work effectively, TIMs must physically conform to the mating surfaces under reasonable assembly pressures and exhibit low contact resistance with adequate bulk thermal conductivity. The bond-line thickness values are kept as low as possible to help reduce bulk thermal resistance; however the thickness must be sufficiently large to enable the TIM to comply with surface irregularities and non-planarities.

Many different TIMs are commercially available that attempt to meet these requirements in different ways. These include a range of adhesives, greases, elastomeric pads, phase-change, carbon and nano-structured materials [1-3]. However, the main weakness of many commercially available TIMs remains their relatively poor thermal performance. Many of these technologies typically consist of a low-conductivity organic phase, such as silicone grease, interspersed with higher conductivity metal (e.g. silver, copper) or ceramic particles (e.g. aluminium oxide, zinc oxide or boron nitride) to enhance the bulk thermal conductivity of the material.

Thermal greases and adhesives are widely used today and are composed of thermally conductive particles dispersed in a fluid matrix. The matrix can be a grease, an adhesive, or an elastomer.

Greases have the lowest viscosity and thus form the thinnest interfaces at a given particle filler loading. Disadvantages of greases include the need for mechanical clamps to maintain contact pressure, creep of material away from the interface over time and/or temperature cycles and poor shelf life due to settling of particles. Adhesives offer permanent assembly, but may more readily trap voids due to their higher viscosity. Elastomers reduce the mess from material creeping away from the bond line, however mechanical clamping is again required. And assembly pressures are higher, especially at large displacements.

In most of these materials (i.e. greases, adhesives and elastomers), the thermal conductivities are relatively low—typically just one order of magnitude better than the organic matrix (100 times lower than pure metals). This is because the organic matrix forms the continuous phase within the materials whereas the thermally conductive particles are discrete and heat transfer is limited by multiple point-to-point contacts between adjacent particles. The limited number of contact points limits the thermal conductivity. For example, despite using extremely high conductivity filler materials, such as silver ($k \approx 420$ W/m·K), the effective thermal conductivity of the best commercially available TIMs is on the order of 3 to 10 W/m·K, which is considerably lower than the thermal conductivities of typical mating components. Significant work has been done in the past to maximize the particle loading and the total particle-to-particle contact area, however additional improvements have been limited due to the maturity of the systems. In addition, dispensing and flow of the particle-matrix composite can result in voids being trapped within the bond.

Pure, soft metal thermal interface materials such as indium are also used. Although the thermal conductivities of these materials are significantly higher than those of metal-organic composites, the ability of these materials to comply with non-flat and high rough surfaces is limited. For some materials, especially indium, fretting corrosion may become a reliability problem, especially where numerous thermal cycles are experienced. Also the relatively low melting point of indium would limit applicability and assembly options

Finally, graphite pads are used extensively in Alcatel-Lucent hardware, particularly in radio frequency power amplifier (RF PA) assemblies off Remote Radio Heads (RRH). These TIMs consist of graphite flakes that are exfoliated by thermally vaporizing an intercalant ion inserted between its layers, generating an internal pressure that causes the intercalated graphite to expand in the direction perpendicular to the layers. The expanded graphite flakes are then mechanically consolidated together with a matrix into a cohesive sheet of flexible graphitic material [4, 5]. The results is a flexible sheet that has a reasonable through-plane thermal conductivity (3-5 W/m·K) [4]. However, due to the highly anisotropic nature of the structure, the in-plane conductivity is significantly higher, ranging from 140 to 500 W/m·K according to Smalc et al. [5]. As a result, they are a viable option for heat spreading applications [5]. However, despite being a flexible sheet and possessing a relatively high thermal conductivity, their thermal performance is limited by the lack of mechanical compliance as they are compressed between surfaces. Even at compressive pressures of 1 MPa, graphite pads exhibit only approximately 5% bulk strain [4]; compliance is more limited when high aspect ratio surface features are present. Furthermore, graphite pads typically lead to an increased electrical contact resistance when assembled between components. For example, when used in certain RF PA applications, poor grounding through these joint results in lowered PA efficiency.

Generally, the bulk thermal conductivities of the thermal interface materials currently used are very low compared to the thermal conductivities of the components being assembled. As a result, the thermal interface between the two components remains the dominant resistance to heat transfer. In many high thermal energy dissipating systems, the TIMs can account for up to 50% of the available thermal budget of the package [6]. With the implementation of high-performance liquid and phase-change cooling strategies, this percentage becomes even greater and thermal interfaces become a critical “bottleneck” to effective cooling. If the thermal management of an electronic device is inadequate, unacceptable temperature levels may be reached which can adversely affect device performance, reliability and lifespan [7]. These thermal issues have spawned a global effort towards the development of exotic TIMs with complex formulations [1-3, 6-9].

2. Metal Micro-Textured Thermal Interface Materials

To address the performance limitations of conventional thermal interface materials, particularly graphite pads used in RRH PA applications, a metal micro-textured thermal interface material (MMT-TIM) has been developed [10, 11]. The concept is illustrated in Fig. 1. These materials consist an array of small-scale (≈0.1 mm to 1 mm) raised features. When this structure is compressed between two mating surfaces, the features plastically deform and conform to the contacting bodies as illustrated in Fig. 1.

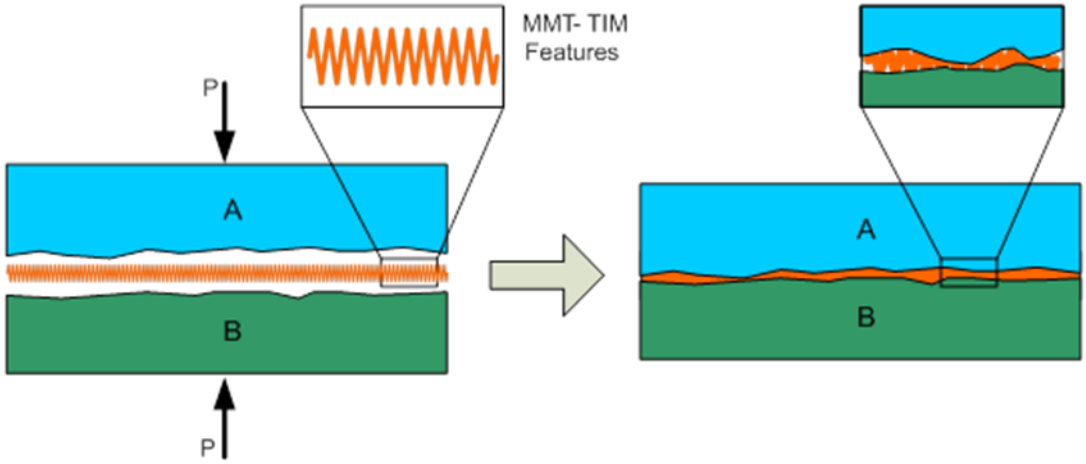

Fig. 1: Metal Micro-Textured Thermal Interface Material Concept

Plastic deformation of the features into the asperities of the contacting surfaces ensures intimate contact with the contacting bodies. The result is an array of conformable, yet continuous solid metal features of low thermal resistance (or high effective thermal conductivity) that are in intimate contact with the mating surfaces due to the plastic deformation of the raised features.

Given the nature of this concept, there is clearly a large design space within which the materials and geometries of the MMT-TIMs could be optimized to minimize thermal resistance and compressive pressure while maximizing mechanical compliance and effective thermal conductivity. Initial investigations into MMT-TIMs explored the effect of size and shape of the raised features on their thermal-mechanical response during compression [10, 11].

Complete thermal-mechanical models which simultaneously characterize the complex feature deformation and effective thermal resistance of MMT-TIMs have been developed to serve as design tools for these materials [12, 13].

The present embodiment of this technology is shown in Fig. 2. In this embodiment, the TIM geometry consists of continuously formed truncated domes approximately 0.5 mm in size extending in both directions from a mid-plane however. This geometry is desirable because it readily allows for buckling and compression when assembled between two components. The open “holes” in the tops and bottoms of the raised features reduce the stiffness of these structures and allow the compression and flow of metal as the entire structure is compressed. These MMT-TIMs were fabricated from flat, 25 µm tin foil using a proprietary micro-stamping operation.

The compressed geometries this MMT-TIM design is shown in Fig. 3. Here the truncated domes have undergone large-scale compressive deformation including bending and buckling modes that results in flattened structures that form a continues path between the assembled bodies including areas that are in intimate contact with the compressing surfaces. This creates highly effective thermal and electrical paths between the mating components.

The objective of the present study is to characterize the thermal performance of a remote radio head (RRH) using the MMT-TIM shown in Fig. 2 installed in the critical interface between the power amplifier (PA) board and the main natural convection heat sink.

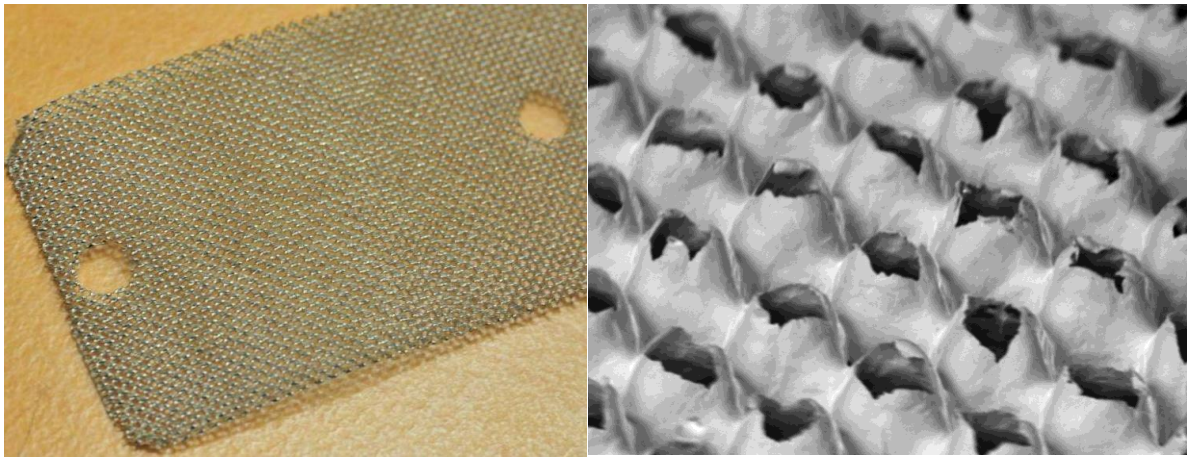

(a) (b)

Fig. 2: a) Photograph and, b) SEM image of a MMT-TIM prior to compression

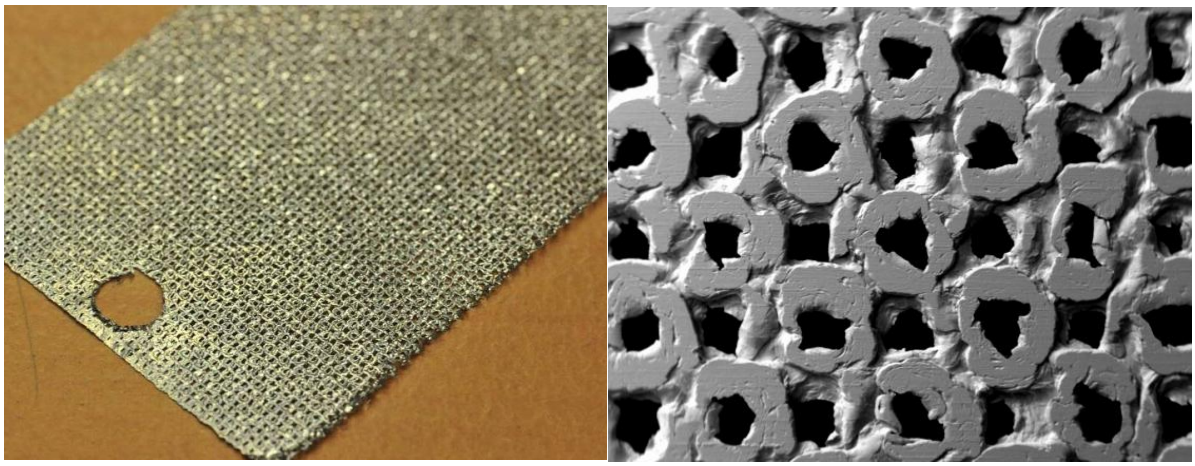

(a) (b)

Fig. 3: a) Photograph and, b) SEM image of a MMT-TIM subsequent to compression

2. Experiment Characterization

A drawing of the RRH in-situ test setup employed in the present study is shown in Fig. 4. The upper part of the RRH consists of a PA heat sink on which the PA board is mounted. Here The PA transistors (shown in red) are the dominant heat-generating components on the PA board (blue). This PA is configured of two main and peak pairs (Doherty configuration). The PA transistors are soldered to a flush mounted copper coin embedded and flush mounted with the bottom of the PCB. These coins serve primary RF ground purpose but do afford some heat spreading. The TIM is between the PA board and the heat sink and an RF shield is mounted over the PA board. Forty M3 screws torqued to 1.0 N·m bolt the RF shield to the heat sink, sandwiching the PCB tightly against the heat sink. Standard screw fasteners and torque patterns were maintained.

The aluminum heat sink is approximately 500 mm tall and 270 mm wide and contains several heat pipes embedded in the base to improve heat spreading. The fins are optimized for natural convection.

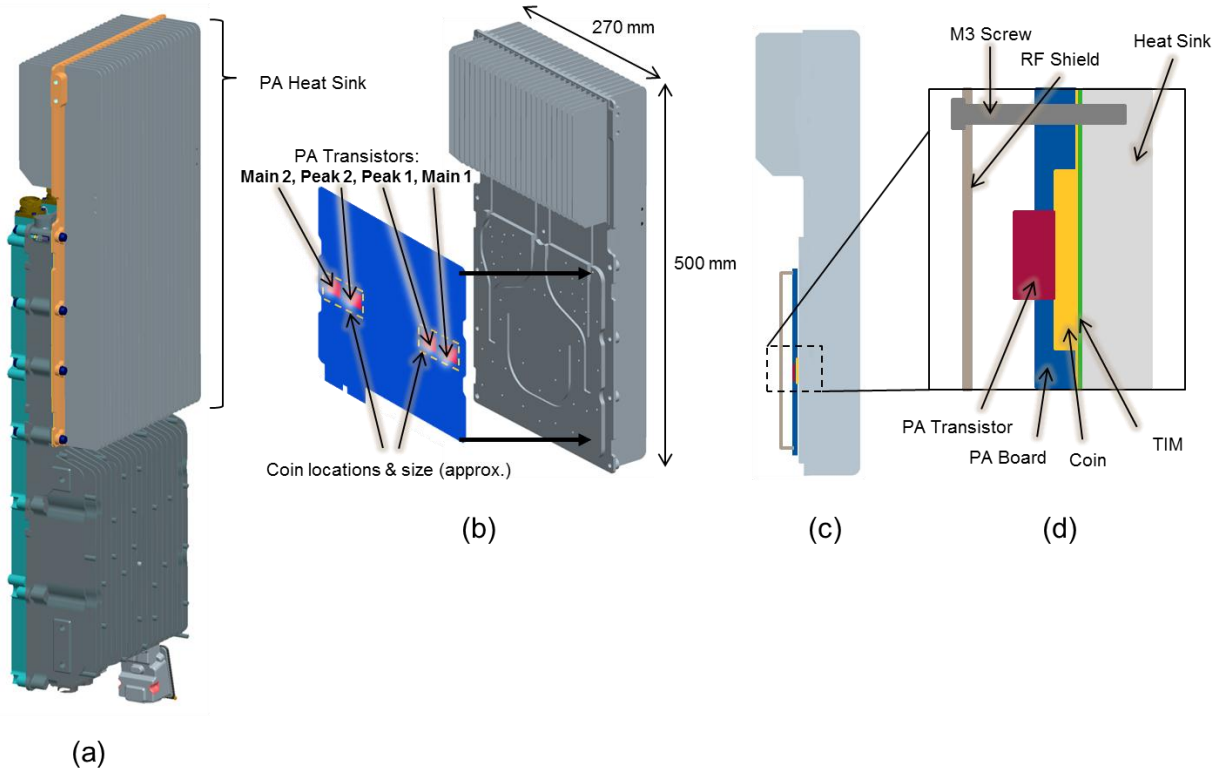

Fig. 4: Drawing of the RRH PA assembly used in the present work a) overall RRH with PA heat sink indicated, b) PA board (transistors in red) and PA contact interface with heat sink, c) side view of assembly showing d) cross-section of assembled component stack-up

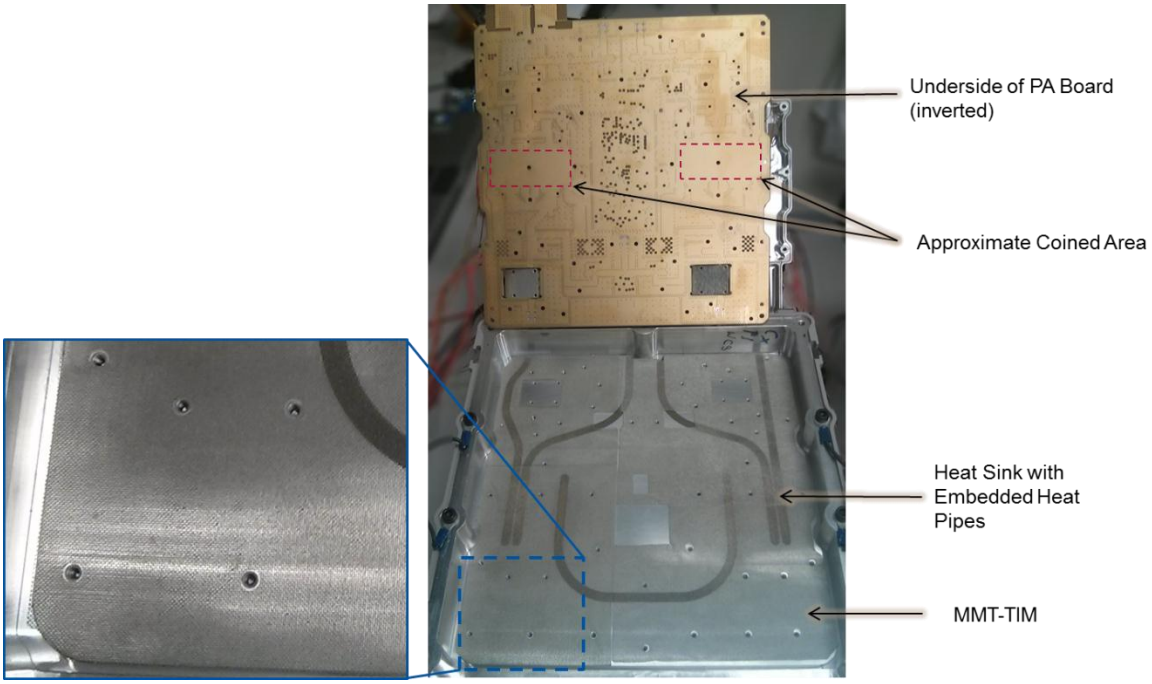

Fig. 5: The heat sink showing embedded heat pipes and the underside of the PA board (inverted relative to the heat sink) with a close up of the MMT-TIM prior to installation

A photograph of the contact area of the heat sink and the underside of the PA board (inverted relative to the heat sink) is shown in Fig. 5. Here the approximate size and shape of the flush-mounted coins in the PA board are indicated. Also visible are the embedded heat pipes in the heat sink base and the MMT-TIM prior to installation.

The outer case of each PA transistor was instrumented with a T-type thermocouple using a high-temperature epoxy. An additional thermocouple was used to measure the ambient air temperature. The required heat load was generated by the transistors themselves by wiring them in a bias mode. Four TTi CPX4000DP DC power supplies provided the operating and bias voltages. The power dissipated by each device was controlled by varying the bias voltage of the circuit and measured by computing the product of the current draw and operating voltage. A fixed power of 81.5 W on the two main devices and 23.6 W on the two peak devices was used. This corresponds to the maximum thermal output of these devices in the field. Ambient temperature was approximately 20 °C.

3. Results & Discussion

Four different interface conditions were tested and compared: i) the PA assembled with no TIM, ii) using a flat, 25 tin foil, iii) the conventionally specified graphite pad , iv) the tin MMT-TIM presented in the previous section. The thermal resistance of this interface (and indeed the system) is difficult to characterize due to the presence of multiple heat sources with thermal communication between them. Consequently, results here are presented using the heat source temperatures rather than thermal resistance.

The steady-state temperature of each device above ambient is shown in Fig. 6 for each of the four interface conditions. As could be expected, using no TIM resulted in the highest observed device temperatures with outer case temperature of Main 1 at 88.5 °C. The conventionally used graphite pad lowered this temperature somewhat while the MMT-TIM resulted in significantly lower device temperatures across the board. For comparison, an un-textured flat Sn foil was also tested as thermal interface material however, only minimal temperature reductions were observed.

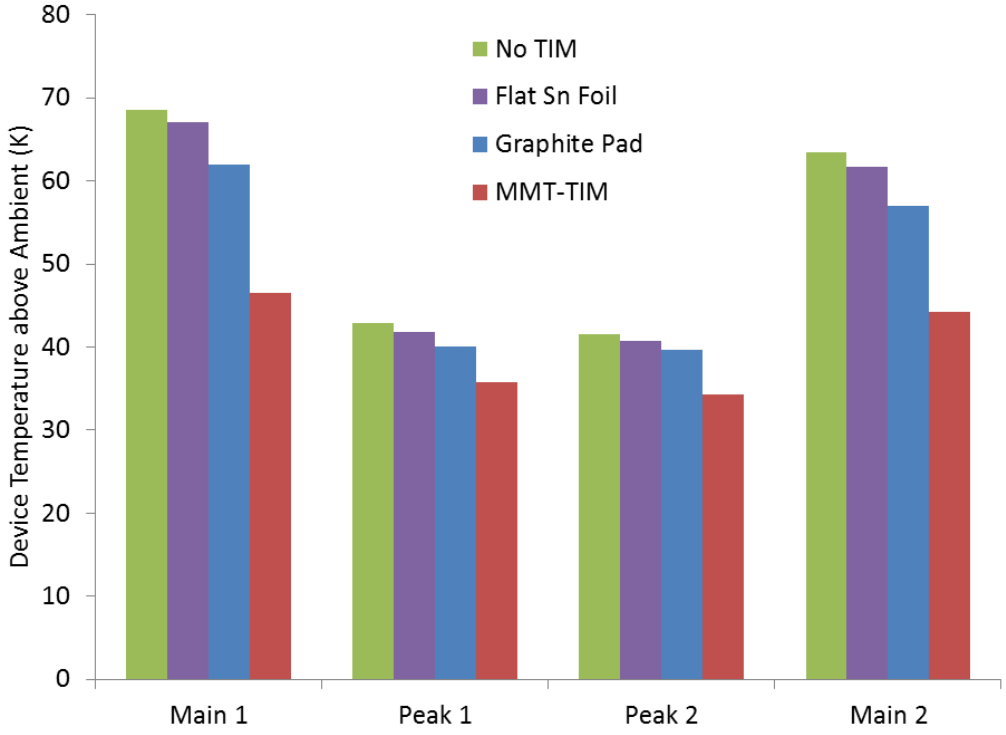

Fig. 6: Device operating temperatures for different TIMs

These tests indicate the interface resistance between the PA board and the heat sink is of crucial importance to the performance of the RRH. For the example of transistor Main 1, the temperature difference between using no TIM and a MMT-TIM is 22 °C—nearly one third of the 68.5 °C temperature difference between of Main 1 and ambient with no TIM.

A more detailed comparison between the conventionally specified graphite pad and the MMT-TIM is shown in Fig. 7. The results indicate clearly that use of the MMT-TIM in place of the graphite pad resulted in a significant drop in terms of absolute device temperatures: The "Main 1" device operating temperature dropped from 81.1 °C to 66.2 °C; a 14.9 °C temperature reduction. The "Main 2" device saw a temperature reduction of 12.2 °C. The temperature reductions in the peak devices were commensurate with their somewhat lower power dissipations: approximately 4.3 and 3.3 °C in "Peak 1" and "Peak 2", respectively.

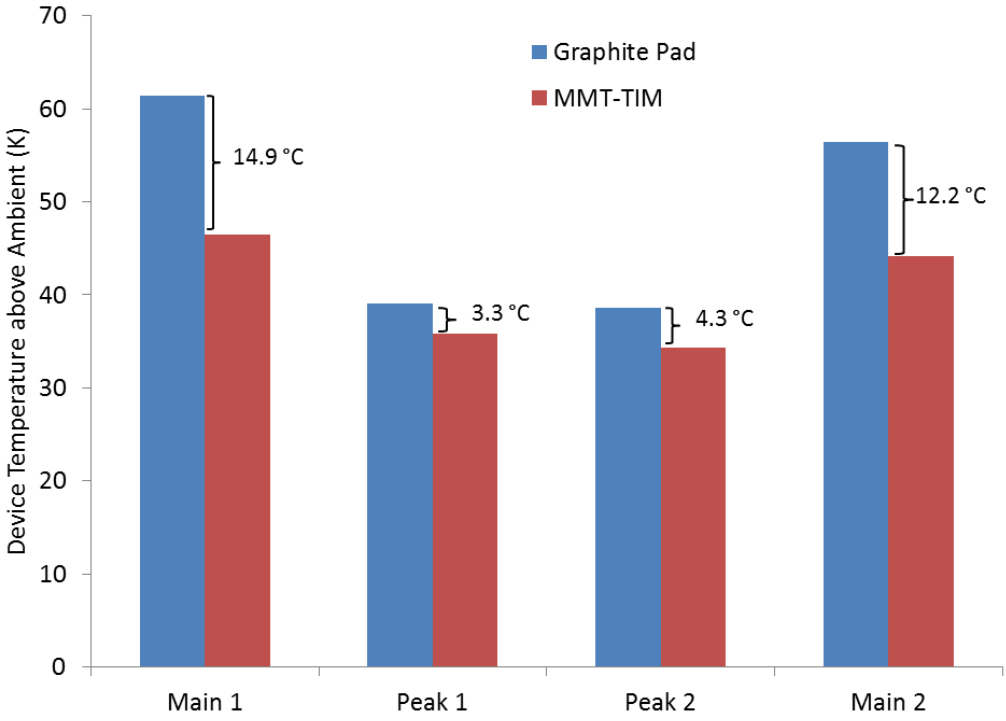

Fig. 7: Detailed comparison between conventional graphite pad and MMT-TIM in terms of resultant device temperatures

The results further illustrate the thermal benefit from using a MMT-TIM in this assembly compared to a conventional graphite pad. This level of temperature reduction has significant implications on overall system design. For example, this level of temperature reduction can have significant positive implications upon device and system reliability. Alternatively, the decreased thermal resistance of this interface can be offset by employing a smaller and lighter heat sink in order to minimize the overall size and weight of the RRH.

The results presented so far characterize the MMT-TIM at shortly after installation at beginning of life. Another crucial aspect is how the TIM performs over time as the assembled interfaces heat up and cool down, expanding and contracting over time. Power cycling tests are recommended for assessing TIM reliability since these tests resemble most closely the actual use of the material [14].

An initial investigation to asses the reliability of the MMT-TIMs in the present application was performed using this setup by alternately powering the four PA transistors between zero and full (rated) power. At each setting the system was allowed to come to steady-state and device temperatures were monitored. The device temperatures at full power (steady-state) are shown in Fig. 8 over 100 power cycles (which took approximately one week). Here no significant changes in device temperature occurred.

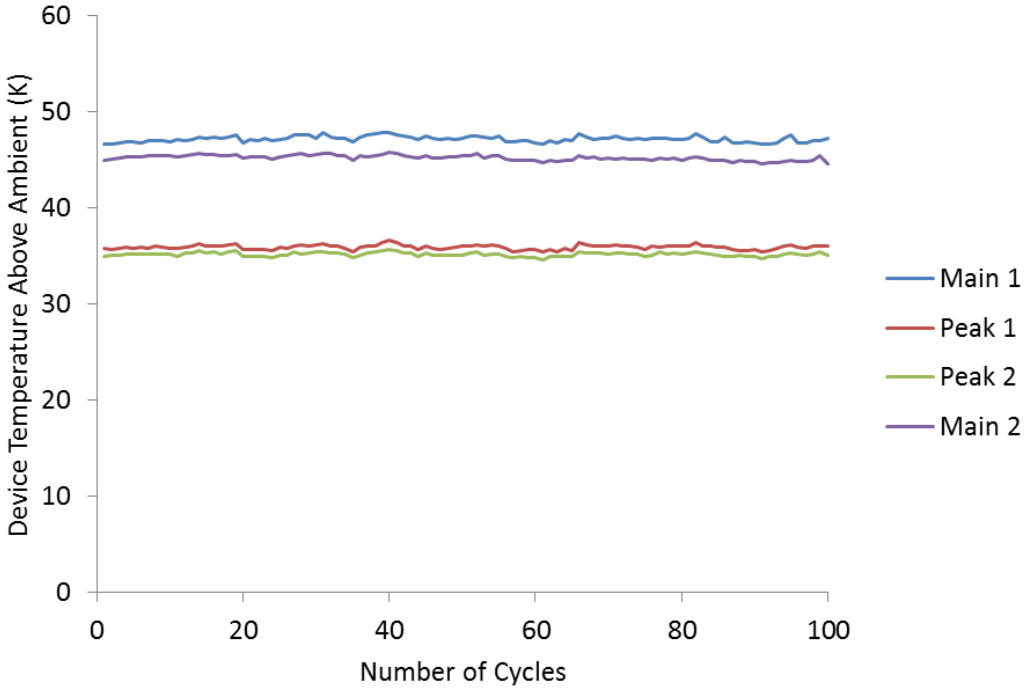

Fig. 8: PA transistor steady-state temperatures during power cycling

4. Conclusions

In-situ tests of a metal micro-textured textured thermal interface material (MMT-TIM) in an RRH PA application have demonstrated a significant reduction in system thermal resistance and therefore device operating temperatures. These temperature reductions will allow for improved system reliability or could be traded off against a smaller heat sink to decrease overall system size and weight.

System power cycling tests were employed to make an initial assessment into the reliability of MMT-TIMs in this application and it was shown that the device temperature remained constant over 100 cycles from zero to full power.

This experimental data will be combined with system-level numerical simulations in order to establish the fractional contribution played by MMT-TIM to the total thermal resistance of the RRH and evaluate possible reductions in heat sink size and weight as a result of lowering the interface resistance.

References

1. Liu, J., Michel, B., Rencz, M., Tantolin, C, Sarno, C., Miessner, R., Schuett, K-V., Tang, X., Demoustier, S. & Ziaei, A., 2008, "Recent Progress of Thermal Interface Material Research—An Overview", Proceedings of the 14th Workshop on Thermal Issues in ICs and Systems (THERMINIC), Rome, Italy, September 24-26, 2008

2. Chung, D.D.L., 2012, "Carbon materials for structural self-sensing, electromagnetic shielding and thermal interfacing", Carbon, 50, pp. 3342 – 3353.

3. McNamara, A. J., Joshi, Y., & Zhang, Z.M., 2012, "Characterization of nanostructured thermal interface materials - A review", International Journal of Thermal Sciences, 62, pp. 2-11, doi:10.1016/j.ijthermalsci.2011.10.014

4. Smalc, M., Norley, J., Reynolds, R.A., Pachuta, R. & Krassowski, D.W., 2013, "Advanced Thermal Interface Materials Using Natural Graphite". Proceedings of the International Electronic Packaging Technical Conference and Exhibition (InterPACK), Maui, USA, July 6-11, 2003.

5. Smalc, M., Shives, G., Chen, G., Guggari, S., Norley, J. & Reynolds, R.A., 2005 "Thermal Performance of Natural Graphite Heat Spreaders". Proceedings of the International Electronic Packaging Technical Conference and Exhibition (InterPACK), San Francisco, USA, July 17-22, 2005.

6. Smith B., Brunschwiler, T., & Michel, B. 2008, "Comparison of transient and static test methods for chip-to-sink thermal interface characterization". Microelectron. J., doi:10.1016/j.mejo.2008.06.079

7. Linderman, R., Brunschwiler, T., Smith B. & Michel, B., 2007, "High performance thermal interface technology overview". Proceedings of the 13th Workshop on Thermal Issues in ICs and Systems (THERMINIC), pp. 129-134.

8. Savija, I., Culham, J.R., Yovanovich, M.M. & Marotta, E.E., 2003, "Review of thermal conductance models for joints incorporating enhancement materials" Journal of Thermophysics and Heat Transfer, 17, pp. 43-52.

9. Nguyen, J. J., Bougher, T. L., Pour Shahid Saeed Abadi, P., Sharma, A., Graham, S. & Cola, B. A., 2013, "Postgrowth Microwave Treatment to Align Carbon Nanotubes" Journal of Micro and Nano-Manufacturing. 1(1), 014501; doi: 10.1115/1.4023162

10. Kempers R., Robinson, A.J. & Lyons, A 2009, "Characterization of Metal Micro-Textured Thermal Interface Materials" Therminic 2009, Leuven, Belgium

11. Kempers, R., Robinson, A. J. & Lyons, A "Characterization of Thermal Contact Resistance in Metal Micro-Textured Thermal Interface Materials using Electrical Contact Resistance Measurements" Defect and Diffusion Forum Vols. 297-301 (2010) pp. 1190-1198. doi:10.4028/www.scientific.net/DDF.297-301.1190

12. Kempers, R., Frizzell, R., Lyons, A. & Robinson, A.J. 2009, "Development of a Metal Micro-Textured Thermal Interface Material" ASME InterPACK 2009, San Francisco.

13. Kempers, R., Lyons, A. & Robinson, A. J. 2014, "Modelling and Experimental Characterization of Metal Micro-Textured Thermal Interface Materials" Journal of Heat Transfer, 136, pp. 011301-1-011301-11DOI: 10.1115/1.4024737

14. Due, J. & Robinson, A.J., 2013, "Reliability of thermal interface materials: A review" Applied Thermal Engineering, **50**, pp.455-463.